Assessment of retinal function and characterization of lysosomal storage body accumulation in the retinas and brains of Tibetan Terriers with ceroid-lipofuscinosis

Martin L. Katz, PhD; Kristina Narfström, PhD, DVM; Gary S. Johnson, PhD, DVM; Dennis P. O'Brien, DVM

Objective—To characterize lysosomal storage body accumulation in the retina and brain of Tibetan Terriers with ceroid-lipofuscinosis and determine whether the disease in these dogs is accompanied by impaired retinal function and retinal degeneration.

Animals—Three 7- to 10-year-old Tibetan Terriers with ceroid-lipofuscinosis and 1 healthy 5-year-old Tibetan Terrier.

Procedure—Owners completed a questionnaire to identify behavioral and physical signs indicative of ceroid-lipofuscinosis. Neurologic, behavioral, and ophthalmologic evaluations, including full-field electroretinograms, were performed on each dog. Fluorescence, light, and electron microscopy were performed on specimens of retina, cerebral cortex, and cerebellum of all dogs postmortem.

Results—Behavioral assessments of the affected dogs revealed moderate visual impairment in low-light conditions but good vision in bright light. On funduscopic evaluation of these dogs, abnormalities detected ranged from none to signs of moderately advanced retinal degeneration. Compared with findings in the control dog, electroretinography revealed depressed rod cell function with some impairment of cone cell function in the affected dogs. Morphologically, disease-specific storage bodies were detected in retinal Müller cells and neurons, particularly in ganglion cells, and in cells of the cerebral cortex and cerebellum in affected dogs. Substantial photoreceptor cell loss and disruption of photoreceptor outer segment morphology appeared to develop late in the disease.

Implications for Human Medicine—The similarities between ceroid-lipofuscinosis in Tibetan Terriers and some forms of ceroid-lipofuscinosis in humans suggest that the canine disease may have a genetic and biochemical basis similar to that of one of the ceroid-lipofuscinosis disorders in humans. (*Am J Vet Res* 2005;66:67–76)

The human **ceroid-lipofuscinoses (CLs)**, also known as neuronal CLs and Batten disease, are a group of inherited neurodegenerative diseases characterized by massive accumulations of autofluorescent lysosomal storage bodies in a variety of cell types, including neurons.[1] In most forms of CL in humans, the onset of clinical signs occurs during childhood; signs include vision loss, seizures, progressive decline in cognitive and motor functions, and premature death.[2] A rare adult-onset type of CL (known as Kufs' disease) is associated with dementia, behavioral problems, and sometimes seizures.[3] Unlike the childhood-onset CLs, Kufs' disease is not characterized by severe vision loss.[3] All forms of CL, other than a subset of the adult-onset type, have an autosomal recessive pattern of inheritance. Mutations in at least 7 distinct genes underlie different variants of the human CLs.[2,4]

Ceroid-lipofuscinosis has been reported in several animal species, including many different dog breeds.[1,5,6] Most reports of CL in dogs involve few or isolated cases within each breed. However, many cases of CL have been identified in Tibetan Terriers, in which the disease appears to be inherited as an autosomal recessive trait.[7] The authors of this report have identified > 25 Tibetan Terriers that appeared likely to have CL on the basis of clinical signs and pedigree analyses and have confirmed the accumulation of autofluorescent lysosomal storage bodies in many of these dogs. The high incidence of CL in this breed can be attributed to 2 factors: the number of dogs in the breed is relatively small, resulting in a high degree of inbreeding, and the onset of clinically apparent signs occurs relatively late, after most dogs have been bred. This makes it difficult to eradicate the disease through selective breeding. Ceroid-lipofuscinosis in Tibetan Terriers could serve as a useful model for one of the human forms of the disease if affected dogs could be bred selectively; however, there is a desire to eradicate CL from the breed among those individuals who breed Tibetan Terriers as pets or for show. Whether one wishes to maintain or eliminate the CL mutation in Tibetan Terriers, it would be highly advantageous to identify affected dogs prior to the onset of behavioral signs, which typically occurs at 4 to 6 years of age. This could be accomplished by use of either DNA markers or early phenotypic markers. The gene defect underlying CL in Tibetan Terriers has not been identified or mapped. However, several

years ago, it was reported that Tibetan Terriers with CL had pronounced changes in the response of the retina to light stimuli (as measured by **electroretinography** [**ERG**]) as early as 7 weeks of age.[7] By 4 to 5 years of age, the ERG response was reported to be barely recordable in affected dogs. Thus, early ERG changes appeared to be a potential early marker for the disorder. However, the pronounced ERG changes that were reported in that study did not appear to be consistent with owner reports that impairment in visually mediated behavior is relatively mild in affected dogs and does not become apparent until 5 years of age or later. The purposes of the study reported here were to characterize lysosomal storage body accumulation in the retina and brain of Tibetan Terriers with CL and determine whether the disease in these dogs is accompanied by impaired retinal function and retinal degeneration. A goal of the research was to identify phenotypic features that could be used to definitively identify affected dogs so that candidate gene and gene linkage analyses could be performed.

Materials and Methods

Animals—With the assistance of the Tibetan Terrier Club of America, phenotypic data, pedigree information, and, when possible, tissue samples have been collected from privately owned Tibetan Terriers over the past several years. Phenotypic data were collected by means of a questionnaire completed by the dog owners. The questionnaire asked the owners to check off on a list the occurrence and severity of behavioral and physical signs that are potentially associated with CL in this breed. There were 33 behavioral and physical signs listed on the questionnaire. Owners were asked to rate their dog as being normal or having mild, moderate, or severe changes for each clinical sign relative to the dog's condition before the onset of signs; they were also asked to indicate whether the changes were continuous or intermittent. With regard to abnormal behaviors of their dogs, respondents were asked to provide narrative descriptions. Dogs were designated as probably affected if the owners indicated that they exhibited at least 6 of the characteristic clinical signs of CL.

When dogs likely to be affected with CL were euthanatized, the authors attempted to obtain samples of brain tissue and the eyes. Tentative diagnoses were confirmed by identification of the characteristic lysosomal storage bodies that accumulate in brains and retinas in association with this disease; to detect the lysosomal storage bodies, specimens were examined by use of fluorescence and electron microscopic techniques. Among 15 potentially affected dogs from which brain tissue and eyes were obtained, we were able to examine 3 dogs to assess whether severe ERG changes are characteristic of CL in the Tibetan Terrier breed. The 3 dogs included a 7-year-old spayed female (dog A), a 9.5-year-old neutered male (dog B), and a 10-year-old spayed female (dog C). Each of the dogs had many of the behavioral signs of CL that develop in this breed. The questionnaires completed by the owners indicated that the 3 dogs had most or all of the following clinical signs that were rated as moderate to severe: loss of housetraining; nervousness; development of aggression toward people; loss of ability to recognize or respond to commands; becomes upset by loud or unfamiliar sounds; walks into walls; loss of ability to jump up onto or down from elevated surfaces (such as chairs); increased stiffness or weakness; difficulty in movement or coordination; impaired ability to see at night; and impaired ability to process visual information (on the basis of the owner's interpretation of changes in visually mediated behavior). In addition, dog B

was reported to have had seizures starting at the age of approximately 9.5 years. The age of onset of the major clinical signs, including visual signs, was reported as 5 to 6 years. Both parents of dog A had behavioral signs of CL, and the diagnosis of CL was confirmed for the dog's dam via examination of the brain and retinas for the characteristic storage material. At the time of the study, the sire of dog A was alive and had the clinical signs of advanced CL. For dogs A and C, euthanasia was planned; the owners permitted neurologic and clinical ophthalmologic examinations and **magnetic resonance imaging** (**MRI**) of the brain to be performed prior to euthanasia and the collection of tissue specimens postmortem. At 9.5 years of age, dog B underwent all of the tests that could be performed antemortem; tissue specimens were collected from this dog after it was euthanatized at 10 years of age.

A clinically normal 5-year-old male Tibetan Terrier was included in the study for comparison with the CL-affected dogs. This control dog had none of the clinical signs of CL, and at necropsy, there was no accumulation of autofluorescent lysosomal storage bodies characteristic of CL in brain tissue or the retinas.

All studies conducted with these dogs were performed with conformity to the principles presented in the US Public Health Service Policy on the Humane Care and Use of Laboratory Animals.

Neurologic and ophthalmologic examinations—All dogs were examined by both a veterinary neurologist (DPO) and a veterinary ophthalmologist (KN). After dogs A and C were received from the owners, they were kept for approximately 1 week with daily attention by caretakers and daily outdoor walks on a leash. Dog B was brought in to the clinic by its owner for the examinations and then returned home. The control dog was housed in the university kennel since the age of approximately 6 months. The dogs were brought to the laboratory separately for observation. While being observed by both the ophthalmologist and neurologist, the dogs were allowed to explore the room and interact with the observers. Each dog then underwent routine neurologic and ophthalmic examinations. Visual behavior was tested first in conditions of dim lighting and then in ordinary room lighting. The dog's ability to navigate a maze was evaluated in both lighting conditions. Vision was also tested by monitoring whether the dog's gaze followed hand motions and cotton balls that were dropped in front of the dog's head in both lighting conditions. Thereafter, the direct and indirect pupillary light reflexes were tested. After instillation of 0.5% tropicamide[a] for pupillary dilatation, the fundus was inspected by use of an indirect ophthalmoscope[b] and the anterior segment of the eye was examined by use of a slit-lamp biomicroscope.[c] Photography of each fundus was performed by use of a digital hand-held fundus camera.[d]

ERG evaluations—After an interval of at least 1 day following the clinical retinal examinations, retinal function was tested via simultaneous bilateral full-field flash ERG according to a recently published protocol for clinical diagnostic ERG in dogs.[8] Prior to and during induction of anesthesia, dogs were kept in conditions of normal room light for at least 45 minutes. The room light level was constant at 400 lux (a mean of measurements taken at 8 different locations around the room) and was the same for all dogs. Anesthesia was induced with propofol administered IV and maintained via isoflurane inhalation. A commercial Ganzfeld ERG system[e] was used in conjunction with a flash photostimulator[f] (flash duration, 10 µs). Response signals were amplified and filtered at 1 to 500 Hz for all recordings except oscillatory potentials, which were filtered at 75 to 500 Hz. Flash ERGs were each recorded as mean responses to at least 4 flashes to

minimize noise. Under scotopic conditions, flash intensities included a dim white flash (−2.0 log **candela** [**cd**] s/m^2) and higher intensity stimuli at 3 different light intensities (0.0, 0.3, and 0.6 log cd s/m^2). For photopic ERG recordings, the animals were light-adapted for 10 minutes under white light at 37 cd/m^2 and then maintained under this light intensity during the recordings. Photopic ERGs were performed with the white light stimulus at an intensity of 0.0 log cd s/m^2 with single flashes at 5.1 Hz, and flicker responses recorded were at 30.1 and 50.1 Hz. Contact lens electrodes[g] were cushioned on the cornea with methylcellulose,[h] and platinum subdermal needle reference and ground electrodes[f] were used. The reference electrodes were placed SC at the base of each ear, and the ground electrode was placed SC at the occiput. Each dog was positioned in sternal recumbency during the recordings, and 3 stay sutures were placed within the conjunctival limbus of each eye to position the globes. After preparation of the dog, the lights were turned off and scotopic ERGs were recorded every 4 minutes during a 20- to 24-minute period to study rod function and the process of dark adaptation. The eyes were then subjected to the brighter white light flashes for stimulation of both rod and cone photoreceptors. Thereafter, ERG recordings were obtained under the photopic conditions for evaluation of the cone system. For visualization of the oscillatory potentials, filtering of the scotopic maximum light intensity flash response was performed.

Examination of the brain via MRI—Four to 6 days after the ERG tests, the brain of each dog was examined via MRI; for the examination, the dog was anesthetized by use of pentobarbital administered IV. By use of an MRI scanner,[i] T1 images without and with contrast enhancement and T2 images were obtained in 3 planes from each dog. The MRI images were evaluated by both a veterinary neurologist (DPO) and a veterinary radiologist.

Tissue collection and analysis—The 4 dogs were euthanatized by use of an overdose of sodium pentobarbital administered IV. The eyes were enucleated and immediately placed in fixative. One eye from each dog was fixed in a solution (pH, 7.4) of 1.5% glutaraldehyde, 1.12% paraformaldehyde, 0.13M sodium cacodylate, and 0.13mM CaCl$_2$ for subsequent electron microscopic analysis.[9] The other eye from each dog was fixed in a solution (pH, 7.4) of 4% paraformaldehyde, 8% sucrose, and 50mM sodium cacodylate for subsequent fluorescence microscopic examination. The corneas, irides, and lenses were quickly removed from each eye. With the eyes immersed in fixative, the vitreous body was removed from the posterior segment of each globe by use of a vitrectomy apparatus.[j] The posterior poles of the eyes were incubated in fixative at approximately 20°C with gentle agitation. In preparation for electron microscopy, eyes were fixed for at least 2 hours. In preparation for fluorescence microscopy, eyes were fixed for 1 hour. A region (centered approx 8 mm from the edge of the optic nerve head) was dissected from the inferior nasal quadrant of each eye. Portions of the eyes to be examined via fluorescence microscopy were placed in 170mM sodium cacodylate (pH, 7.4), and portions of the eyes to be examined via electron microscopy were returned to the fixative solution. After two 15-minute washes in the cacodylate buffer, the samples for fluorescence microscopy were incubated for 30 minutes first in a solution of 10% sucrose in cacodylate buffer and then in a solution of 20% sucrose in cacodylate buffer; samples were further incubated for 30 minutes in a 1:1 mixture of 20% sucrose and optimal cutting temperature solution.[k] Finally, the samples were incubated in optimal cutting temperature solution for 45 minutes and frozen on dry ice.

After a minimum of 4 hours in the fixative, the samples for electron microscopy were processed for embedding in epoxy resin by use of established procedures. Specimens were washed in 170 mM sodium cacodylate (pH, 7.4) prior to secondary fixation in 1% osmium tetroxide. Subsequently, the fixed samples were dehydrated through immersion in a graded series of acetone solutions and were embedded in epoxy resin. Sections of the embedded samples were cut for both light and electron microscopic examinations. For light microscopy, sections mounted on slides were stained with toluidine blue. For electron microscopy, sections were stained with uranyl acetate and lead citrate and examined by use of a transmission electron microscope.[l]

The brains were removed intact within 10 minutes of the time of euthanasia. A razor blade was used to cut approximately 3-mm-thick slices of the cerebral cortex and cerebellum from near the superior midline. Samples to be used for electron microscopy were placed in the same fixative as that used for the eyes, incubated with gentle agitation for a minimum of 2 hours at approximately 20°C, and processed according to the protocol used for the eye tissue samples. Samples of brain for fluorescence microscopy were fixed and embedded in optimal cutting temperature solution in the same manner as the eye tissue samples.

A cryostat was used to cut sections of the frozen samples at a thickness of 7 μm. Sections were mounted on glass slides and examined and photographed by use of a microscope equipped for epifluorescence illumination.[m] Fluorescent emissions were stimulated with light from a 50-W, high-pressure mercury-vapor source. Samples were examined and photographed by use of a 40X objective lens[n] with a 1.30 numerical aperture, a 395- to 440-nm bandpass exciter filter, an FT 460 chromatic beam splitter,[n] and an LP 515 barrier filter.[n] Photography was performed by use of daylight-balanced color slide film.[o]

Retina samples that were obtained from the inferior-nasal quadrant of each eye and processed for electron microscopy as described were used to assess cell nuclei densities in the inner and outer nuclear layers. Sections of the embedded samples (centered approx 4 mm from the edge of the optic nerve head) were cut at a thickness of 1 μm, mounted, and stained with toluidine blue. Photographs of these sections were obtained at a magnification of 400X, and the number of cells/100 μm of retina length (measured along the retinal pigment epithelium) was determined for each dog. Counts were performed on at least 3 sections from each eye, and the mean retinal length per section analyzed was 280 μm. Morphologic analyses were performed in a masked fashion by a single observer (MLK).

Results

As indicated by responses to the questionnaire completed by the owners, all 3 dogs had behavioral signs previously identified as characteristic of CL in this breed; key behavioral, neurologic, and ophthalmologic abnormalities and their severity (relative to clinically normal dogs or these same dogs earlier in life) as reported by the owners and observed during veterinary examination were recorded. Dogs A, B, and C had signs of nervousness to some degree (moderate, mild, and severe, respectively), and all were aggressive toward people. Problems with house soiling were moderate in dogs A and C, but no such problems were reported for dog B. Owners reported that all 3 dogs had reduced vision in dim light; in bright light, vision appeared by the owners to be reduced only in dogs A and B.

In dogs A and B, gait was moderately ataxic with occasional stumbling and crossing over of limbs; the ataxia was more severe in dog C, which often fell over

and then had difficulty getting back on its feet. There was also some degree of hypermetria in the forelimbs in these dogs. In all 3 dogs, stance was wide-based; proprioceptive positioning was brisk, but hopping and hemiwalking were abnormal, especially in the forelimbs. Dogs A and C responded aggressively when picked up for visual placing but placed accurately. Dog C had considerable muscle atrophy, particularly in the hind limbs; this dog would often turn its head from side to side repeatedly when standing still. Appetite was good in all 3 dogs; however, dog C had difficulty eating and drinking from a bowl and had to be given food and fluids by hand during the last few days of its life. There were no deficits on cranial nerve examinations in any of the dogs except for slow pupillary light reflexes. Myotactic reflexes were normal in dogs A and B but depressed in dog C. Forelimb withdrawal response was weak, whereas hind limb withdrawal appeared normal. The results of the neurologic examination suggested diffuse cerebral disease with cerebellar involvement in all 3 dogs, whereas dog C also had signs of peripheral nerve involvement.

With respect to visual behavior, all 3 dogs could negotiate obstacles in the examination room but occasionally bumped into objects, especially in low-light conditions. The dogs appeared to track falling cotton balls and hand motions normally in both visual fields in ordinary room lighting but more inconsistently in the dark. A normal palpebral reflex was elicited in response to rapid hand motions in both visual fields, primarily in bright light. In the 3 affected dogs, both direct and indirect pupillary reflexes were slower than they were in the control dog and slight mydriasis was present throughout the testing procedure. There was no evidence of any ocular condition other than retinal degeneration that could

account for the mydriasis in the affected dogs. In dog A, no abnormalities were detected in either eye via biomicroscopy or ophthalmoscopy (**Figure 1**). In dog B, moderately advanced generalized retinal degeneration was observed. Dog C had a central fundus of normal appearance, but there was a slight increase in tapetal reflectivity in the midperipheral fundic area as well as some attenuation of the retinal blood vessels peripherally.

Results of the ERG analyses indicated substantial functional impairment in the affected dogs. Under identical testing conditions in all 4 dogs, comparison of b-wave amplitudes measured in the affected animals with those obtained from the control dog revealed that the mean reduction in rod cell function in the dogs with CL was 80% (**Table 1**; **Figure 2**). Conversely, cone cell function was not impaired in the affected dogs.
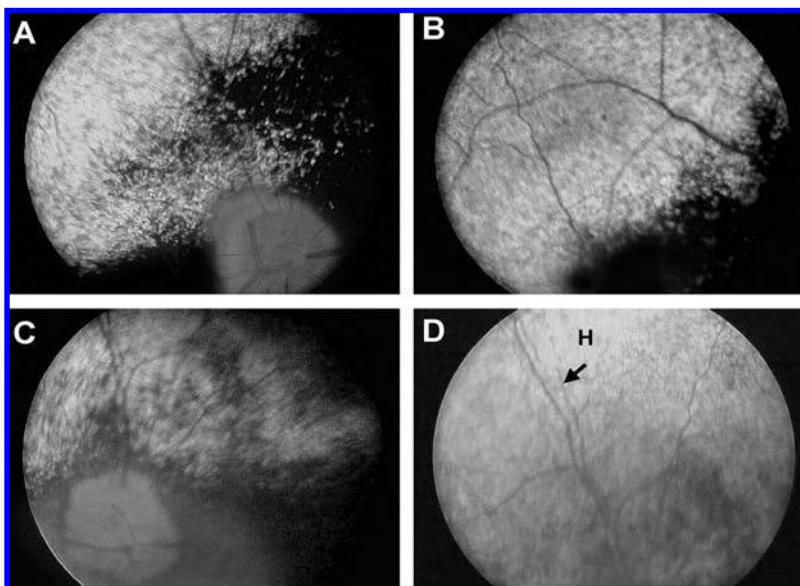

Figure 1—Results of ophthalmoscopic examination of 2 Tibetan Terriers with ceroid-lipofuscinosis (CL). A and B—Central and peripheral areas of the fundus of dog A, respectively. C and D—Central and peripheral areas of the fundus of dog C, respectively. In panel D, notice the vascular attenuation (arrow) and tapetal hyperreflectivity (H). Fundic changes in dog C were difficult to photograph clearly because of age-related nuclear sclerosis of the lens.

Table 1—Electroretinographic (ERG) response amplitudes and implicit times obtained under various stimulus conditions in 3 Tibetan Terriers with ceroid-lipofuscinosis and an unaffected control dog of the same breed.

| Variable	Control dog	Dog A	Dog B	Dog C
Age (y)	5	7	9.5	10
Phenotype	Normal	Affected	Affected	Affected
ERG response amplitude (µV)				
Scotopic low-intensity b-wave	110	34	18	13
Scotopic high-intensity b-wave	125	85	38	42
Scotopic high-intensity a-wave	85	37	28	32
Photopic high-intensity b-wave	25	17	31	30
Photopic high-intensity a-wave	8	5	6	8
Photopic flicker	32	22	34	38
ERG response implicit times (ms)				
Scotopic low-intensity b-wave	75	60	65	66
Scotopic high-intensity b-wave	33	35	36	32
Scotopic high-intensity a-wave	15	12	13	11
Photopic high-intensity b-wave	28	27	28	28
Photopic high-intensity a-wave	12	11	12	13
Photopic flicker	25	25	22	23
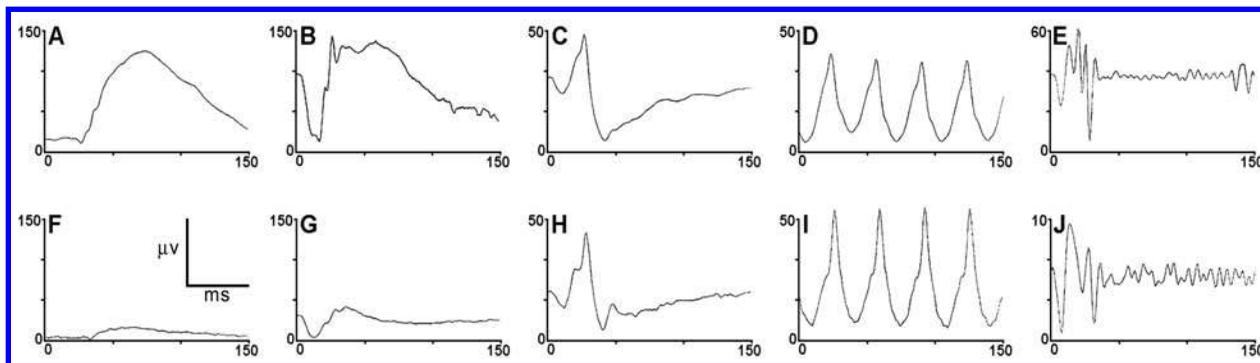
Figure 2—Results of electroretinographic (ERG) recordings in a 5-year-old control Tibetan Terrier not affected with CL (A through E) and a 9.5-year-old CL-affected dog B (F through J). In the 2 dogs, testing was performed with scotopic low-intensity light stimuli (–2 log candela [cd] s/m^2; A and F); scotopic high-intensity light stimuli (0.3 cd s/m^2; B and G); and photopic stimuli (0.0 log cd s/m^2) at 5.1 (C and H) and 30.1 Hz (D and I). Oscillatory potentials (E and J) were obtained for each dog by filtering the scotopic maximum response at 0.6 cd s/m^2 of light intensity at 75 to 500 Hz. Units for axes are shown in panel F (inset); notice the difference in vertical axis scale between panels E and J.

Compared with values in the control dog, implicit times for the scotopic b-wave responses to low-intensity stimuli were decreased by a mean of 11 milliseconds in the affected dogs; the timings of all of the other responses recorded were within normal limits. Oscillatory potentials were markedly reduced in amplitude in all affected animals (Figure 2). During a 20-minute period of dark adaptation, the b-wave amplitude response of the control dog to a constant intensity stimulus increased by 189% from 38 to 110 μV (**Figure 3**). In the 9.5- and 10-year-old dogs (dogs B and C), the increases in b-wave amplitudes were only approximately 5 and 8 μV, respectively, but on a percentage basis, these increases of 200% and 133% were similar to that detected in the control dog. The 7-year-old affected dog (dog A), which had a b-wave amplitude that was only slightly lower than that of the control dog at the start of the dark adaptation period, had an increase of only 8 μV during the 20-minute period of dark adaptation, compared with an increase of 73 μV for the control dog during the same period.

Magnetic resonance imaging of the brains of the dogs with CL revealed moderate dilatation of the ventricles suggestive of generalized brain atrophy. No focal lesions or signs of other causes of the neurologic signs in the CL-affected dogs were observed in any brain area. The MRI appearance of the control dog brain was normal; neither focal nor diffuse abnormalities were observed.

Examination of cerebral cortex samples via fluorescence microscopy revealed massive amounts of autofluorescent inclusions in the cortical neurons of all 3 affected dogs (**Figure 4**). Electron microscopic examination revealed substantial accumulations of electron-dense inclusion bodies in the perinuclear regions of cerebral cortical neurons (**Figure 5**). The cerebellum also had a very large amount of autofluorescent inclusion material, particularly in the Purkinje cell layer. Electron microscopic examination revealed that the perinuclear cytoplasm of most Purkinje layer cells contained many large inclusion bodies that were filled with what appeared to be whorls of membrane-like material (**Figures 6 and 7**). In comparison, other cells in the Purkinje cell layer contained inclusions that were
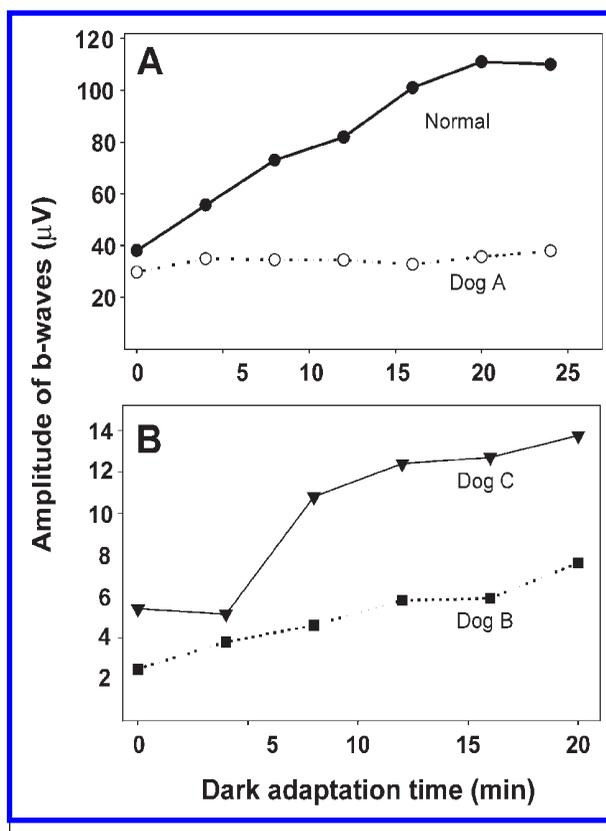

Figure 3—Plots of the ERG response amplitudes at a constant flash intensity as a function of duration of dark adaptation for the control dog and the 7-year-old CL-affected dog A (A) and for the 9.5- and 10-year-old CL-affected dogs B and C (B). Notice the differences in amplitude scales between panels A and B.

smaller and had a distinctly different ultrastructural appearance. Cells in the granule cell layer of the cerebellum contained storage bodies similar to those observed in the cerebral cortex. Autofluorescent inclusions were also observed in retinal neurons, particularly in the ganglion cells (Figure 4); the retinal inclusions contained whorls of membrane-like material similar to that observed in some brain neurons (**Figures 8 and 9**). Although the ultrastructural appearances of the storage

bodies differed somewhat among tissues, a common feature in all tissues examined was the presence of membrane-like material within the storage bodies.

With the exception of the presence of inclusion bodies in the inner retinal neurons, light microscopic examination of retinal sections from dogs A and C revealed that the gross morphology of the neural reti-
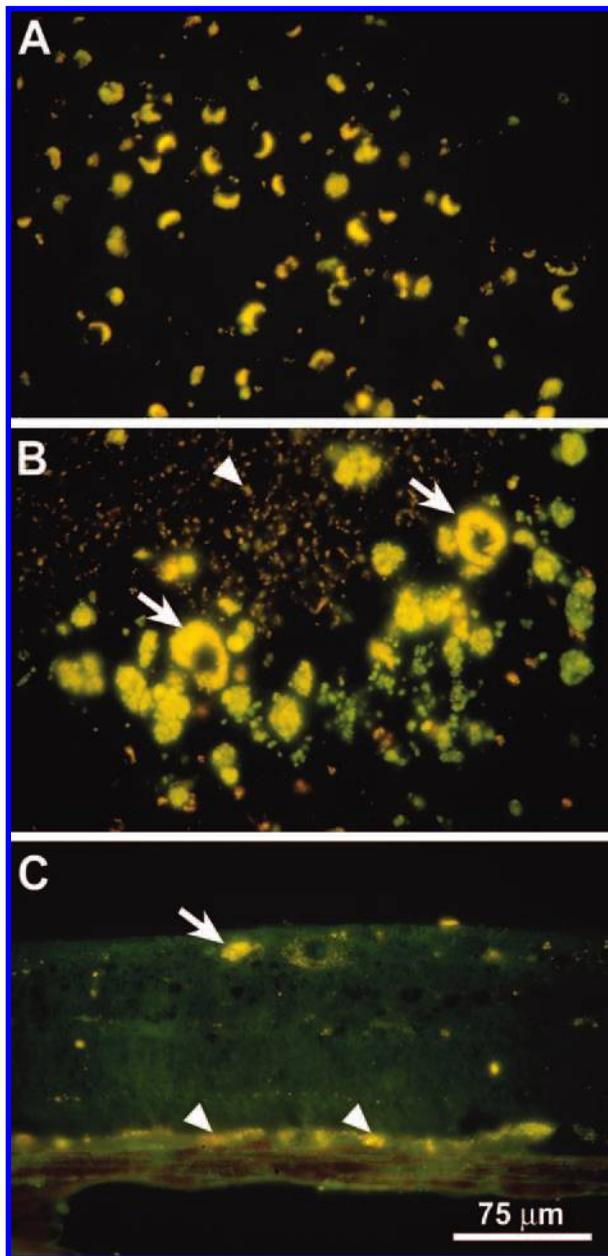
nas was fairly normal at both the posterior pole and in the peripheral regions (**Figure 10**). However, compared with findings in dogs A and C, the outer nuclear layer was dramatically thinned and there was a shortening of the photoreceptor outer segments in dog B. Quantitative analyses of the number of nuclei in the inner and outer nuclear layers of the retina indicated
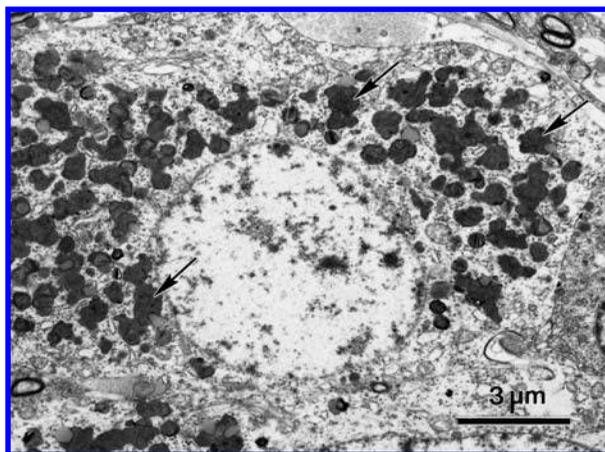

Figure 5—An electron micrograph of a cerebral cortical neuron from the CL-affected dog A. Notice the large number of inclusion bodies (arrows) in the perinuclear region of the cell.

Figure 4—Fluorescence micrographs of cryostat sections of cerebral cortex (A), cerebellum (B), and retina (C) from CL-affected dog A. The golden yellow fluorescence is characteristic of the storage material that accumulates in cells in dogs with CL. A— Cells containing large amounts of storage material are present throughout the cerebral cortex. B—In the cerebellum, the cells with the large inclusions (arrows) are primarily in the Purkinje cell layer, whereas the cells with the smaller inclusions (arrowhead) are in the granular cell layer. C—In the retina, the presence of autofluorescent inclusions in the neural retina (arrow) is unique to CL, whereas autofluorescent pigment accumulation in the retinal pigment epithelium (arrowheads) develops during normal aging. Bar in panel C indicates the magnification for all 3 micrographs.
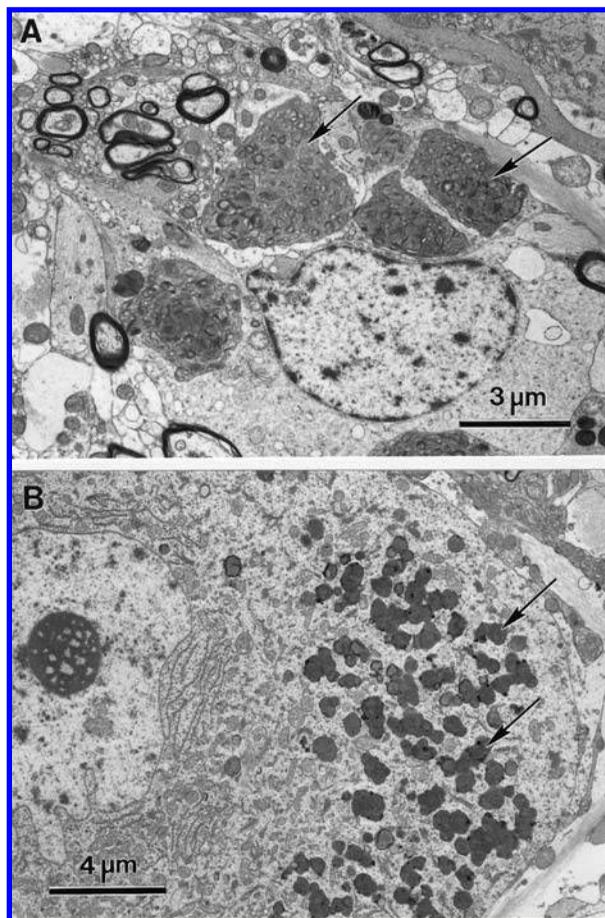

Figure 6—Electron micrographs of cells in the Purkinje cell layer (A) and the granule cell layer (B) of the cerebellum of CL-affected dog A. Notice the distinctive morphologic appearance of the storage bodies (arrows) that accumulate in these cell layers.
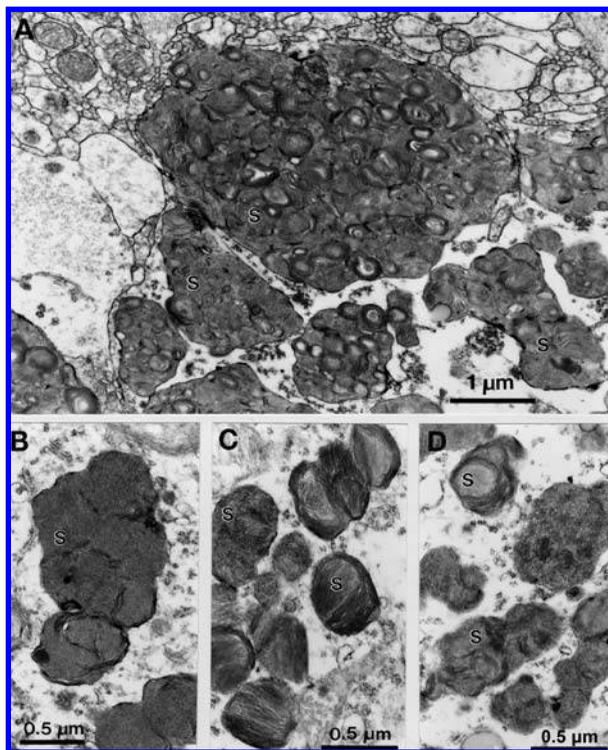
Figure 7—Electron microscopic appearance of storage bodies (S) in cells of the Purkinje cell layer (A and B) and granule cell layer of the cerebellum (C) and gray matter of the cerebral cortex (D) of CL-affected dog A. Notice that in the Purkinje cells, there are 2 morphologically distinct types of storage bodies: large inclusion bodies composed primarily of closely packed whorls of membrane-like material (A) and smaller inclusions containing mostly granular-appearing material (B). Note that the sizes and morphologic appearance of the storage bodies also differ among brain regions. A common feature of the storage bodies is that they all contain at least some membrane-like inclusions.
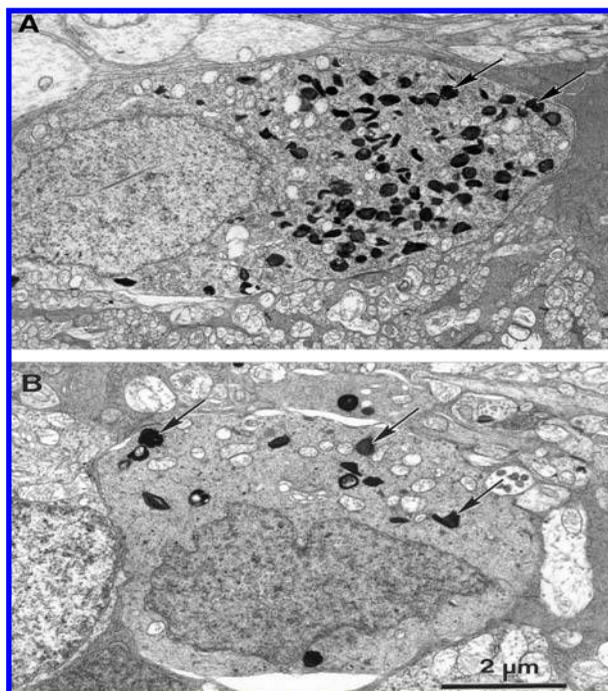

Figure 8—Electron microscopic appearance of storage bodies (arrows) in a ganglion cell (A) and in a Müller cell (B) from the retina of CL-affected dog A. Bar in (B) indicates magnification for both micrographs.
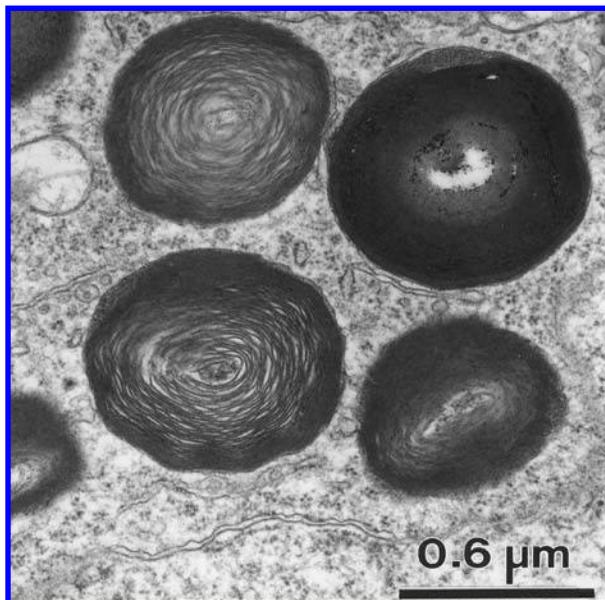

Figure 9—Electron micrograph of storage bodies in a ganglion cell from the retina of CL-affected dog A. Notice the whorls of membrane-like contents similar to storage bodies observed in some brain neurons of the affected dogs.
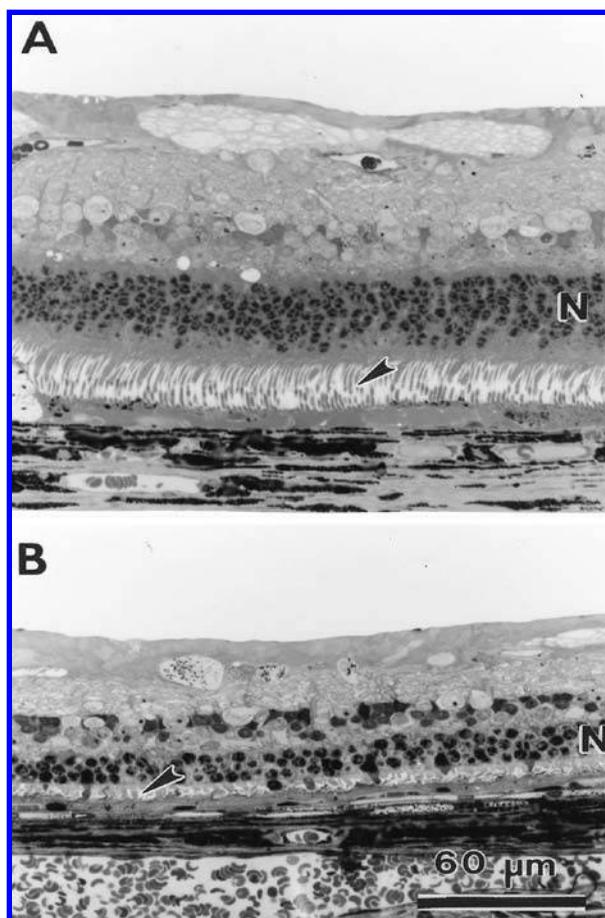

Figure 10—Photomicrographs of the inferior central areas of the retinas of CL-affected dog A (A) and dog B (B). Notice the difference in the degree of retinal degeneration between these 2 dogs; compared with findings in dog A, the outer nuclear layer (N) and photoreceptor inner and outer segment lengths (arrowheads) are greatly decreased in dog B. Bar in panel B indicates the magnification for both micrographs.
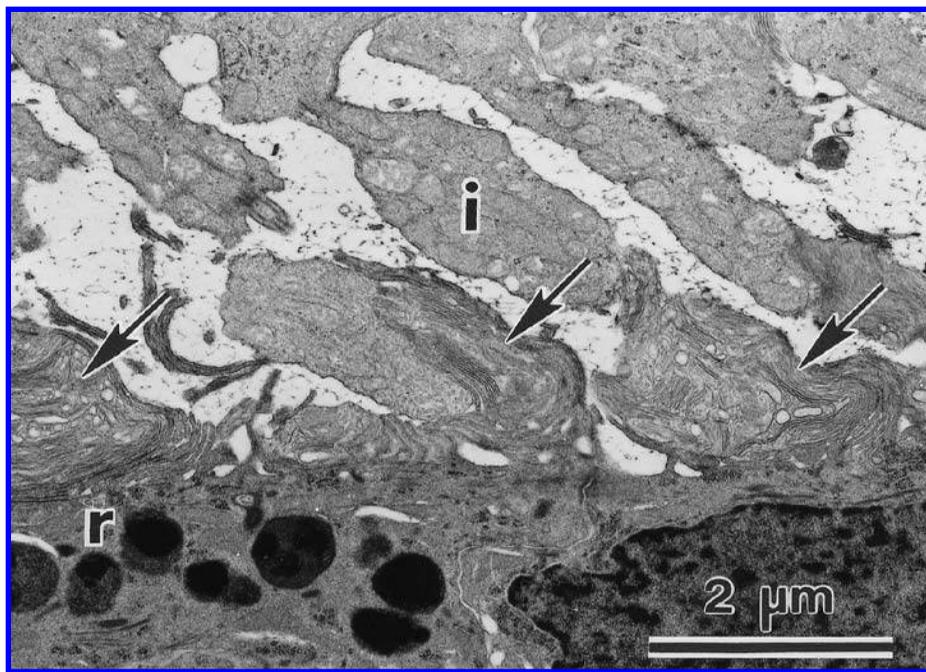
Figure 11—Electron micrograph illustrating the degenerated condition of the photoreceptor outer segments in the inferior nasal retinal area in dog B. No normal outer segments were observed in this region of the retina, only occasional small stacks of what appeared to be abnormal outer segment disk membranes (arrows); image includes photoreceptor inner segments (i) and an apical portion of a retinal pigment epithelial cell (r).

that all 3 affected dogs had decreased photoreceptor cell densities in 1 or both layers, compared with values in the control dog. In dogs A, B, and C, the number of nuclei/100 μm of the inner nuclear layer of the retina was 45, 33, and 44, respectively; cell density in the inner nuclear layer of the retina was 43 in the control dog. In dogs A, B, and C, the number of nuclei/100 μm of the outer nuclear layer of the retina was 125, 40, and 87, respectively; cell density in the outer nuclear layer of the retina was 159 in the control dog. Electron microscopic examination of retinal sections obtained from dog B (the most severely affected dog with respect to ERG responses) revealed a complete absence of normal photoreceptor outer segments; only a small number of abnormal and shortened outer segments remained (**Figure 11**).

Discussion

In the 7- to 10-year-old Tibetan Terriers with CL that were examined in the present study, both dark- and light-adapted ERG responses were reduced in amplitude and had modified waveforms under some stimulus conditions, compared with those obtained under similar recording conditions from a clinically normal 5-year-old Tibetan Terrier. However, both dark- and light-adapted ERG responses were easily recordable in all 3 affected dogs. In a previous report,[7] early-onset ERG changes were suggested to be characteristic of CL in Tibetan Terriers; it was reported that severe ERG abnormalities could be observed in affected dogs as early as 7 weeks of age. By the time the dogs were 4 to 6 years of age or older, the ERG response was barely detectable. This finding is in pronounced contrast to that of the present study, in which easily recorded ERG

responses were obtained from even the oldest and most severely affected dog. In the previous study,[7] the disease was reported to be accompanied by a loss of cells from the inner retinal layers by 3 years of age, although no data were presented to support that conclusion. In our study, a modest loss of cells with nuclei in the inner nuclear layer was observed only in one of the 10-year-old dogs with CL, indicating that degeneration of this layer is a relatively late manifestation of CL in Tibetan Terriers. Photoreceptor cell degeneration was also previously reported in CL-affected dogs, but the age of onset and severity of this sign were not provided.[7] Among the dogs examined in the study of this report, loss of photoreceptor cells from the inferior nasal region of the central portion of the retina (compared with findings in a 5-year-old control dog) was approximately 20% in the 7-year-old dog and 45% and 75%, respectively, in the 2 older dogs. These data correlated well with the ERG findings. It appears that photoreceptor cell loss with accompanying loss of retinal sensitivity is probably a late manifestation of CL in these dogs and progresses slowly. The differences in severity of retinal signs between the two 10-year-old dogs suggested that environmental and genetic variations may modify the phenotypic expression of the disease-causing mutation.

In any of the hereditary CLs, the relationship between lysosomal storage body accumulation and cell death is not understood. In the Tibetan Terriers of the present study, photoreceptor cell loss was substantial despite the apparent absence of storage body accumulation in these cells or in the supporting retinal pigment epithelium. It is possible that the genetic defect that results in CL causes a disruption of an important function in photoreceptor cells without causing storage body formation in those cells. Alternatively, cells of the inner retina may exert a trophic effect on the photoreceptors and that effect is impaired when inner retinal neurons accumulate the storage material. Clearly, more research needs to be done to elucidate the relationship between storage body accumulation and degenerative changes in the nervous system.

In the affected dogs of our study, there appeared to be decreases in the implicit times for the scotopic low-intensity b-wave and the scotopic high-intensity a-wave, compared with the values obtained in the control dog. However, additional clinically normal dogs should probably be examined to determine the normal

range of ERG implicit times for this breed. The onset of the a-wave represents the onset of photoreceptor response, whereas the peaks of the a- and b-waves are determined by a combination of the photoreceptor response and the summed responses of cells in the inner retina. Thus, the timing of these peaks is determined by the relative amplitudes of the photoreceptor and inner retinal responses. The decreased scotopic low-intensity b-wave implicit time, compared with that of the control dog, suggests a decrease in the ratio of rod cell to inner retinal response amplitudes measured under these conditions, which is consistent with a loss of rod photoreceptor cells. The apparent decreased scotopic high-intensity a-wave implicit time in the CL-affected dogs (compared with that in the control dog) is consistent with a decrease in the ratio of rod cell plus cone cell to inner retinal response amplitudes measured under these conditions. Under scotopic conditions, the photoreceptor response amplitude is determined primarily by rod cells; thus, the decreased scotopic high-intensity a-wave implicit time also probably reflects primarily decreased rod cell input to the ERG.

Owners of CL-affected dogs usually report impairments in visual function in dim light, with either more moderate or no impairment in bright light. This is consistent with the findings of behavioral assessments performed in the laboratory on the 3 affected dogs examined in our study. In bright room light, all 3 of the dogs responded normally to a variety of visual stimuli, whereas in dim light, visual performance was impaired. The behavioral observations correlated well with the ERG findings, suggesting that rod photoreceptor-mediated vision deteriorates in Tibetan Terriers with CL, whereas cone cell function is well preserved.

In the central inferior portion of the retinas of the affected dogs, pronounced losses of photoreceptor cells and a paucity of normal photoreceptor outer segments were detected, compared with findings in the control dog. Despite this morphologic evidence of degeneration, the cone cell ERG responses in the affected dogs were similar to those of the 5-year-old clinically normal Tibetan Terrier, whereas rod responses were substantially reduced. These data suggest that rods are preferentially affected in development of this disorder.

Until the disease is quite advanced, the expected decreases in ERG amplitudes in Tibetan Terriers with CL would usually not be detected via a typical clinical screening ERG in which rod cell and cone cell functions are not typically separated.[10,11] Indeed, an ERG analysis was performed in another clinic by a veterinary ophthalmologist on a 6-year-old Tibetan Terrier that had clinical signs of CL but was not included in our study. In that dog, ERG flash and flicker responses were recorded at a single stimulus intensity; under the conditions of the analysis, the ERG responses were within the normal range for dogs. Nevertheless, that dog was later confirmed to have CL at necropsy. In that instance, a more elaborate type of ERG analysis that separates rod cell and cone cell functions, such as that performed in the present study, might have been useful in the diagnosis of CL. Analyses of young dogs, followed by disease status confirmation, will be needed to assess the value of the ERG analysis in the identification of affected dogs before behavioral signs develop. However, ERG amplitudes that are decreased from normal values alone cannot be used to identify affected dogs because other disorders, particularly eye-specific diseases such as progressive retinal atrophy and congenital stationary night blindness, can result in decreased ERG responses. Indeed, progressive retinal atrophy has been reported in Tibetan Terriers[12] and it is unlikely that ERG analysis alone could distinguish between progressive retinal atrophy and CL. It is possible that dog B of the present study (that had the most severe retinal degeneration of the 3 affected dogs examined) had both progressive retinal atrophy and CL.

In addition to reduced ERG rod cell responses, compared with those of the control dog, the youngest affected dog in our study had little relative increase in retinal sensitivity during dark adaptation; under the same conditions, the response amplitude increased by approximately 189% in the clinically normal dog. This impairment of dark adaptation in the CL-affected dog reflects a selective decline in rod cell function. All 3 affected dogs in our study had a marked decrease in oscillatory potentials, compared with the value in the control dog. These oscillatory potentials are complex responses of the inner retina, presumably generated in the region of the amacrine cells, which may be attenuated as a result of the accumulation of inclusion bodies in inner retinal neurons that impairs cell function without resulting in cell death. Our data suggest that in addition to the use of the clinical diagnostic ERG protocol, in which rod cell and cone cell functions are separated and the process of dark adaptation is evaluated, analysis of oscillatory potentials may be useful for identification of dogs affected with CL.

Although the ERG amplitudes observed in the affected dogs examined in the present study were decreased, compared with those of the control dog, these decreases were relatively moderate in comparison with those previously reported in Tibetan Terriers with CL.[7] It is possible that the dogs analyzed by Riis et al[7] had a mutation in a gene that was distinct from any of the CL genes, and it was that which led to early-onset loss of retinal function in those dogs. The dogs examined by those investigators were bred from 1 affected pair,[p] so all of the dogs in that pedigree were likely to carry the same mutations. In the general Tibetan Terrier population, CL would segregate independently from genes that would specifically exacerbate the retinal effects of CL (unless the underlying mutations were on the same chromosome); consequently, only a small fraction of the dogs with CL would also have early-onset loss of retinal function. Thus, it is likely that the early ERG changes reported by Riis et al[7] would only be diagnostic for CL in a subpopulation of dogs. It would be difficult to identify the specific genetic factors responsible for the observed differences in severity of the retinal involvement (as indicated by ERG response amplitudes) in Tibetan Terriers with CL.

In the CL-affected Tibetan Terriers evaluated in the present study, the fluorescence properties and ultrastructural appearances of the neuronal storage bodies observed in retinal and brain tissues were similar to those observed in various forms of CL in humans. In

the dogs, the storage bodies detected in both brain and retinal specimens contained membrane-like inclusions similar to the so-called fingerprint profiles and curvilinear bodies reported in some of the CLs in humans.[2,13-16] However, the ultrastructural features of the storage bodies in the dogs were distinct among different cell types, something that is not often acknowledged in studies of CL in humans.[15] Differences in ultrastructural appearance of storage bodies among different cell types have been reported in English Setters with CL.[17,18] These differences in appearance may reflect differences in the compositions of storage body contents or in the environments in which the materials accumulated.

Ceroid-lipofuscinosis in Tibetan Terriers is a potential model for CL disorders in humans. The late onset of clinical symptoms, accumulation of autofluorescent lysosomal storage bodies in the brain and retinal ganglion cells,[16,19] behavioral changes, and relatively mild visual impairment associated with CL in Tibetan Terriers suggests that the disorder may be analogous to Kufs' disease in humans.[3] However, it is also possible that CL in Tibetan Terriers is a result of a mutation in an ortholog of one of the genes involved in the development of childhood CLs in humans. There are clearly species differences in disease phenotype resulting from mutations in orthologous genes. For example, mice with a mutation in one of the CL genes (CLN3) have much milder pathologic retinal changes than those observed in humans with CLN3 gene mutations.[20] The canine orthologs of the known CL genes in humans may be potential candidates for the CL gene in Tibetan Terriers.

It has been reported that the storage bodies that accumulate in many forms of CL in humans contain the subunit c protein of mitochondrial ATP synthase.[21-24] Results of preliminary studies have indicated that the storage bodies from the cerebella of affected Tibetan Terriers do not contain appreciable amounts of this protein. The mechanisms that underlie the accumulation of subunit c protein in some forms of CL are not known; therefore, the absence of large amounts of this protein in storage bodies from Tibetan Terriers does not rule out the possibility that the canine disease and one of the CLs in humans have a common genetic basis.

References

1. Jolly RD, Palmer DN. The neuronal ceroid-lipofuscinoses (Batten disease): comparative aspects. *Neuropathol Appl Neurobiol* 1995;21:50–60.

2. Wisniewski KE, Kida E, Golabek AA, et al. Neuronal ceroid lipofuscinoses: classification and diagnosis. In: Wisniewski KE, Zhong N, eds. *Batten disease: diagnosis, treatment, and research.* New York: Academic Press Inc, 2001;1–34.

3. Kida E, Golabek AA, Wisniewski KE. Cellular pathology and pathogenic aspects of ceroid lipofuscinosis. *Adv Genet* 2001;45:35–68.

4. Mole SE. Batten's disease: eight genes and still counting? *Lancet* 1999;354:443–445.

5. Jolly RD, Palmer DN, Studdert VP, et al. Canine ceroid-lipofuscinosis: a review and classification. *J Small Anim Pract* 1994;35:299–306.

6. Wrigstad A, Nilsson SE, Dubielzig R, et al. Neuronal ceroid lipofuscinosis in the Polish Owczarek Nizinny (PON) dog. A retinal study. *Doc Ophthalmol* 1995;91:33–47.

7. Riis RC, Cummings JF, Loew ER, et al. Tibetan terrier model of canine ceroid lipofuscinosis. *Am J Med Genet* 1992;42:615–621.

8. Narfström K, Ekesten B, Rosolen S, et al. Guideline for clinical electrophysiology in the dog. *Doc Ophthalmol* 2002;105:83–92.

9. Katz ML, Parker KR, Handelman GJ, et al. Effects of antioxidant nutrient deficiency on the retina and retinal pigment epithelium of albino rats: a light and electron microscopic study. *Exp Eye Res* 1982;34:339–369.

10. Aguirre G. Electroretinography—are we misusing an excellent diagnostic tool? *Vet Comp Ophthalmol* 1995;5:2–3.

11. Narfstrom K. Electroretinography in veterinary medicine—easy or accurate? *Vet Ophthalmol* 2002;5:249–251.

12. Millichamp NJ, Curtis R, Barnett KC. Progressive retinal atrophy in Tibetan Terriers. *J Am Vet Med Assoc* 1988;192:769–776.

13. Boustany RN, Alroy J, Kolodny EH. Clinical classification of neuronal ceroid lipofuscinosis subtypes. *Am J Med Genet Suppl* 1988;5:47–58.

14. Dyken PR. Reconsideration of the classification of the neuronal ceroid-lipofuscinoses. *Am J Med Genet Suppl* 1988;5:69–84.

15. Goebel HH, Zeman W, Patel VK, et al. On the ultrastructural diversity and essence of residual bodies in neuronal ceroid-lipofuscinosis. *Mech Ageing Dev* 1979;10:53–70.

16. Martin JJ, Libert J, Ceuterick C. Ultrastructure of brain and retina in Kufs' disease (adult type of ceroid-lipofuscinosis). *Clin Neuropathol* 1987;6:381–394.

17. Goebel HH. Retina in various animal models of neuronal ceroid-lipofuscinosis. *Am J Med Genet* 1992;42:605–608.

18. Koppang N. English setter model and juvenile ceroid-lipofuscinosis in man. *J Med Genet* 1992;42:594–599.

19. Berkovic SF, Carpenter S, Andermann F, et al. Kufs' disease: a critical reappraisal. *Brain* 1988;111:27–62.

20. Seigel GM, Lotery A, Kummer A, et al. Retinal pathology and function in a Cln3 knockout mouse model of juvenile neuronal ceroid lipofuscinosis (Batten disease). *Mol Cell Neurosci* 2002;19:515–527.

21. Sadzot B, Reznik M, Arrese-Estrada JE, et al. Familial Kufs' disease presenting as a progressive myoclonic epilepsy. *J Neurol* 2000;247:447–454.

22. Sakajiri K, Matsubura N, Nakajima T, et al. A family with adult type ceroid lipofuscinosis (Kufs' disease) and heart muscle disease: report of two autopsy cases. *Intern Med* 1995;34:1158–1163.

23. Palmer DN, Fearnley IM, Walker JE, et al. Mitochondrial ATP synthase subunit c storage in the ceroid-lipofuscinoses (Batten disease). *Am J Med Genet* 1992;42:561–567.

24. Hall NA, Lake BD, Dewji NN, et al. Lysosomal storage of subunit c of mitochondrial ATP synthase in Batten's disease (ceroid-lipofuscinosis). *Biochem J* 1991;275:269–272.